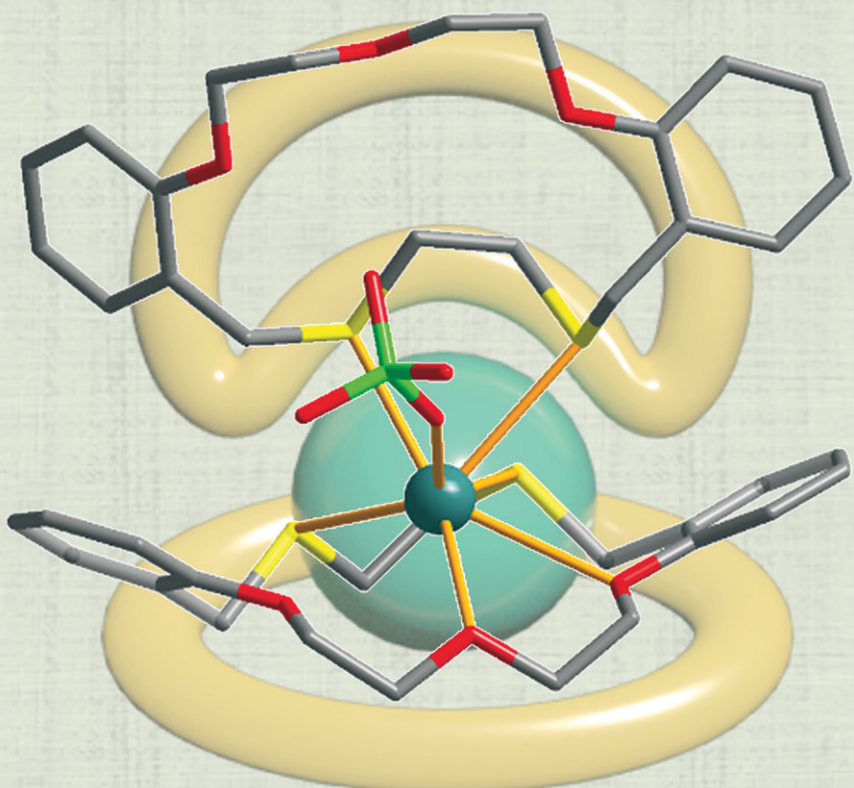


# CrystEngComm

[rsc.li/crystengcomm](http://rsc.li/crystengcomm)



ISSN 1466-8033



Cite this: *CrystEngComm*, 2025, **27**, 1529

Received 12th October 2024,  
Accepted 24th November 2024

DOI: 10.1039/d4ce01045k

[rsc.li/crystengcomm](http://rsc.li/crystengcomm)

**An unsymmetrically sandwiched bis( $O_3S_2$ -macrocycle) lead(II) complex via an endo/exo-coordination mode†**

Seulgi Kim, \* Kyunghye Ju, Taehun Kim and In-Hyeok Park \*

**Abstract** An unsymmetrically sandwiched complex was isolated from the reaction of  $O_3S_2$ -macrocycle with lead(II) perchlorate. The lead(II) centre is bound to one macrocycle in an endocyclic (face) mode and the other in an exocyclic (edge) mode, resulting in a di-capped trigonal prismatic geometry. The edge-to-face sandwich complex might be associated with the hemispherical lead(II) coordination.

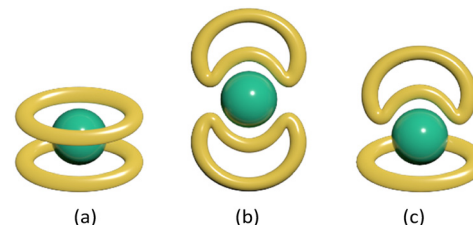
Metal-ligand interactions play a crucial role in the design and functional control of metal complexes, metal-organic frameworks (MOFs), and various macromolecular compounds.<sup>1–11</sup> The precise regulation of such interactions can impart unique chemical properties and reactivities, making crown ethers and their derivatives notable for their ability to selectively bind metal ions.<sup>12,13</sup> Crown ethers have attracted much attention due to the preferential endocyclic (metal-in-cavity) complexation with alkali and alkali earth metal ions in a *good fit* mode.<sup>14</sup> Sometimes, crown ether-type macrocycles form unusual stoichiometric complexes including sandwich types with a 1:2 (metal-to-ligand) ratio, club sandwiches (2:3) and higher-ordered ones.<sup>15–23</sup> In general, sandwich-type complexes are formed when the cavity is relatively small to fully accommodate the metal ion.

On the other hand, various modifications of crown ethers including donor atoms allow new reactivities and functionalities.<sup>24–26</sup> Thiacrowns (or thiamacrocycles), for example, form not only endocyclic complexes but also exocyclic (a metal ion binds outside of the cavity) coordination products due to the preferential *exo*-orientation of sulfur donors.<sup>27–32</sup> Interestingly, the *exo*-coordination between sulfur donors (soft

base) and thiophilic metal ions (soft acid)<sup>33</sup> so often provides an opportunity to construct diverse types of metallosupramolecules from monomers and cyclic oligomers to polymers as reviewed by the Lee group.<sup>34–36</sup> In addition, some controllable *endo*- and *exo*-coordination modes<sup>37,38</sup> and their applications in preparing  $Cu_nI_n$  ( $n = 2$  or 4) clusters,<sup>39</sup> photochemical sensors<sup>40–43</sup> and chiral inversion<sup>44</sup> have been reported.

Considering the contribution of the *exo*-coordination, the sandwich-type macrocyclic complexes could be extended to three types (A–C in Scheme 1, see Fig. S1†) depending on the combination of the *endo*- (face) and *exo*-coordination (edge). Undoubtedly, type A (*face-to-face*) is the most common because large alkali metal ions tend to form this symmetrical sandwich.<sup>15–23</sup> Types B and C involve the *edge* mode, which appears in the *exo*-coordinated soft metal complexes of thiamacrocycles.<sup>34–38</sup> In particular, type C (*edge-to-face*) complexes are unsymmetrical because one macrocycle has most of the donors coordinated in the same plane, while one part of the donors in the other macrocycle participates in the coordination environment. Thus, isolating type C complexes is challenging, especially in a one-pot reaction.

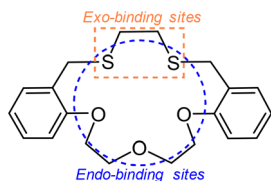
More recently, we have reported a 17-membered  $O_3S_2$ -macrocycle (**L** in Scheme 2) as one of the ditopic model ligands together with its interdonor (sulfur-to-sulfur) distance-dependent *cis*-palladium(II) complex and infinite one-dimensional copper(II) complex.<sup>45,46</sup> Due to three consecutive



**Scheme 1** Sandwich-type macrocyclic complexes with different coordination modes: (a) type A (*face-to-face*), (b) type B (*edge-to-edge*) and (c) type C (*edge-to-face*).

Graduate School of Analytical Science and Technology, Chungnam National University, Daejeon 34134, South Korea. E-mail: sgkim7495@gmail.com, ipark@cnu.ac.kr

† Electronic supplementary information (ESI) available: Synthetic details, characterization, NMR titration, and crystal structure data. CCDC 2389314 (1). For ESI and crystallographic data in CIF or other electronic format see DOI: <https://doi.org/10.1039/d4ce01045k>



**Scheme 2** Chemical structure of a ditopic  $O_3S_2$ -macrocycle (**L**).

oxygen donors, **L** has a hard base nature for *endo*-binding with hard or borderline metal ions (Scheme 2). Meanwhile, two sulfur donors could act as soft bases for the *exo*-binding sites with soft metal ions. In the present work, we employed the ligand **L** to gain a further understanding of non-soft metal complexations.

We have extended such sandwich-type complexes of macrocycles with hard and soft metal ions to borderline metal ions including lead(II) because their complexation behaviours are important in coordination chemistry, materials science and biological areas.<sup>47,48</sup> Lead(II) may bind to both oxygen and sulfur donors in **L** with variable coordination numbers and unusual coordination geometries. Practically, plenty of hemidirected lead(II) complexes involving both Pb–O and Pb–S bonds have been reported so far.<sup>49–55</sup> In this work, we have isolated an unsymmetrically sandwiched lead(II) complex of **L** with an *edge-to-face* mode (type C in Scheme 1) as the first non-soft metal species in this category. The details of our investigations are presented below.

The  $O_3S_2$ -macrocycle **L** was prepared as described previously.<sup>37</sup> One-pot reaction of **L** in dichloromethane with  $Pb(ClO_4)_2 \cdot 3H_2O$  in acetonitrile afforded a colourless crystalline product **1** after slow evaporation at room temperature (yield 32%). X-ray analysis revealed that **1** crystallises in the monoclinic space group  $P2_1/n$  (Table S1†). Product **1** features a 1:2 (metal-to-ligand) complex of type  $[Pb(L)_2(ClO_4)]ClO_4 \cdot 0.5CH_2Cl_2 \cdot 0.5CH_3CN$  that involves one coordinated anion in the complex part (Fig. 1a). The asymmetric unit contains one formula unit.

In **1**, as shown in Fig. 1a, the complex part  $[Pb(L)_2(ClO_4)]^+$  comprises an unsymmetrical sandwich structure in which both *endo*-dentate (**L**<sub>A</sub>) and *exo*-dentate (**L**<sub>B</sub>) macrocycles are bonded to the lead(II) centre in an *edge-to-face* mode (type C in Scheme 1c). The lead(II) centre is eight-coordinated with one macrocycle (**L**<sub>A</sub>) bound to one side of the metal ion *via* the  $O_3S_2$  donors ( $Pb1\text{--}S1$  2.902(13),  $Pb1\text{--}S2$  2.990(12),  $Pb1\text{--}O1$  2.854(3),  $Pb1\text{--}O2$  2.806(3),  $Pb1\text{--}O3$  2.951(1) Å). Interestingly, the coordination sphere is completed by two *exo*-dentate sulfur donors ( $Pb1\text{--}S3$  2.902(11),  $Pb1\text{--}S4$  3.100(12) Å) from the other macrocycle **L**<sub>B</sub> in an *edge* mode and one perchlorate oxygen atom ( $Pb1\text{--}O8$  2.781(9) Å).

The eight-coordinated geometry of **1** can be best described as a distorted di-capped trigonal prismatic geometry (Fig. 1b). The trigonal faces of the prism are defined by S1–S2–S3 and O1–O2–O8. One sulfur atom (S4) and one oxygen atom (O3) cap the corresponding rectangular faces (S1–S3–O8–O1 and S2–S3–O8–O2). Thus, the capping bond lengths of

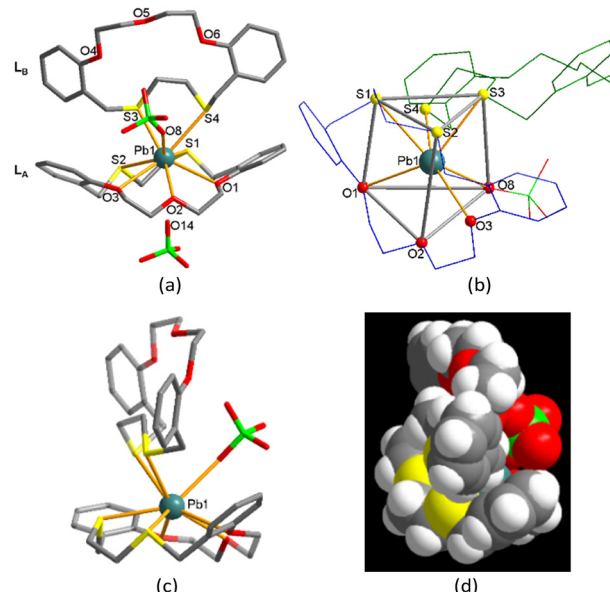


**Fig. 1** An unsymmetrically sandwiched lead(II) complex,  $[Pb(L)_2(ClO_4)]ClO_4 \cdot 0.5CH_2Cl_2 \cdot 0.5CH_3CN$  (**1**): (a) front view, (b) coordination environment of the lead(II) centre, showing a distorted di-capped trigonal prismatic geometry, (c) side view and (d) space-filling structure. Non-coordinated solvent molecules are omitted. Each non-coordinated perchlorate ion in (b-d) is not shown.

$Pb1\text{--}S4$  (3.100(12) Å) and  $Pb1\text{--}O3$  (2.951(1) Å) are slightly longer than those of other  $Pb1\text{--}S$  (2.902(11)–2.990(12) Å) and  $Pb1\text{--}O$  (2.781(9)–2.854(3) Å) bonds, respectively. Similar to the Pb–S bonds (2.902 (11)–3.100(12) Å), the Pb–O<sub>ether</sub> bond lengths (2.806(3)–2.951(1) Å) fall in the longer part of the literature range for such bonds (2.5–2.9 Å).<sup>56</sup> The elongated bond lengths seem to be caused by the steric hindrance between two macrocycles. Also, these are the typical signs of a hemidirected complex discussed in the latter part.<sup>49–55</sup>

Notably, the lead(II) centre is located 1.00 Å above the average plane of the  $O_3S_2$  donors in **L**<sub>A</sub> with a perching manner (Fig. 1c). In general, the perching position in the sandwich-type macrocyclic complexes is mainly due to the larger size of metal ions compared to the macrocyclic cavity. In **1**, however, the perching position of the lead(II) centre is mainly caused by the *exo*-coordination of the macrocycle **L**<sub>B</sub> that lifts the lead(II) centre. Unlike the *face-to-face* mode, which shields the metal centre effectively from anions and solvent molecules, the *edge-to-face* mode in **1** allows some open metal space between the two macrocycles (Fig. 1c and d). Due to this reason, one  $ClO_4^-$  ion participates to the coordination environment ( $Pb1\text{--}O8$  2.781(9) Å), with another  $ClO_4^-$  ion remaining uncoordinated ( $Pb1\cdots O14$  3.243(6) Å) (Fig. 1a). The IR spectrum for **1** shows an intense  $ClO_4^-$  peak at 1045 cm<sup>-1</sup> (Fig. S6†).

As mentioned, lead(II) often shows a hemidirected coordination sphere.<sup>49–55,57</sup> Indeed, the eight-coordinated  $O_4S_4$  coordination environment in **1** occupies only one hemisphere keeping the other hemisphere unoccupied except for the lone pair electron (Fig. 2). In our previous work, the

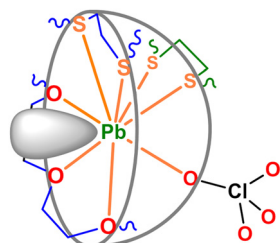


Fig. 2 The hemispherical coordination mode of the eight-coordinated lead(II) centre in **1**.

assembly reactions of lead(II) and zinc(II) with a mixture of the rod-like 1,4-bis(4-pyridyl)piperazine and V-shaped 4,4'-sulfonyldibenzoic acid generate a polyrotaxane and a polycatenane, respectively.<sup>54</sup> In this case, interestingly, the polyrotaxane formation is attributed to the hemisphere configuration of the lead(II) centre. The Penner-Hahn and Godwin groups reported the hemisphere coordination of lead(II) with thiol-rich peptides, which do not induce protein folding unlike the zinc(II)-analogue, as the origin of the lead poisoning.<sup>58</sup> Considering the coordination numbers, elongated bond lengths, anion coordination and steric configuration, the formation of unsymmetrical sandwich-type complex **1** might be responsible for the hemispherical coordination of the lead(II) centre. To the best of our knowledge, this is the first example of unsymmetrically sandwiched macrocyclic complexes with non-soft metal ions. When the analogue product with the soft metal ion shown in Fig. S1c† is involved, this is the second example in the Type C category (Scheme 1c).

For the understanding of the complexation behaviours of **L** with lead(II) perchlorate in solution, we attempted NMR and ESI-mass experiments. In the <sup>1</sup>H NMR titration, the addition of lead(II) (0–1.7 equiv.) to **L** induced all of the proton peaks to shift downfield, reflecting a stable complexation with an exchange rate being fast on the NMR time scale (Fig. 3a and

S3†). The titration curves show that the magnitudes of the chemical shifts follow the order  $H_4 > H_3 \gg H_2 > H_1 > H_{\text{ar}}$  (Fig. 3b). The larger shifts for  $H_4$  and  $H_3$  than those for  $H_2$  and  $H_1$  indicate the more favourable binding of lead(II) to sulfur donors than oxygens. Above 1.0 equiv., no significant chemical shifts were observed probably due to the predominant formation of a 1:1 product in this region.

The stability constant of the complexation was obtained by HyperNMR software (Fig. S4†).<sup>59</sup> This complexation could not be described using a mixed model of the 1:1 and 1:2 ratios (metal-to-ligand). Instead, a good fit of the data with the 1:1 model yields the  $\log K$  value of  $5.9 \pm (0.5)$ , indicating the formation of a typical endocyclic mononuclear lead(II) complex, unlike the crystal structure. It is not surprising that the crystal structure differs from that in solution because of the solvation of the lead(II) with acetonitrile, a dipolar aprotic solvent.

Alternatively, ESI-mass spectroscopy is quite sensitive in monitoring labile or less stable supramolecules assembled in solution. The ESI-mass spectrum of **L** with 1.0 equiv. of lead(II) perchlorate was dominated by peaks for the 1:1 (metal-to-ligand) complexes such as  $[\text{Pb}(\text{L})(\text{ClO}_4)]^+$  ( $m/z$  683) and  $[\text{Pb}(\text{L})(\text{AN})_2(\text{ClO}_4)]^+$  ( $m/z$  765, AN =  $\text{CH}_3\text{CN}$ ) (Fig. 4). In the same spectrum, the formation of both 1:2 and 2:2 complexes is also confirmed by the peaks for  $[\text{Pb}(\text{L})_2(\text{ClO}_4)]^+$  ( $m/z$  1059) and  $[\text{Pb}_2(\text{L})_2(\text{ClO}_4)_3]^+$  ( $m/z$  1465), respectively. This result indicates that the 1:2 stoichiometric species is less stable than in the solid state probably due to the influence of the solvation.

In summary, an unsymmetrically sandwiched 1:2 (metal-to-ligand) complex with an *edge-to-face* mode *via exo/endo*-coordination was isolated from the reaction of a ditopic  $\text{O}_3\text{S}_2^-$ -macrocycle **L** with lead(II) perchlorate. In its crystal structure, the lead(II) centre in a hemisphere configuration adopts an eight-coordinated di-capped trigonal prismatic geometry with the elongated Pb–O and Pb–S bond distances matched to satisfy the steric and electronic conditions required. In solution, the mononuclear bis(macrocycle) product was traced by ESI-mass spectroscopy but such evidence was not observed in the <sup>1</sup>H NMR titration probably due to the solvation effect. The knowledge of such a sandwich-type complex is expected to provide insight into the lead(II) coordination found in biosystems and materials.

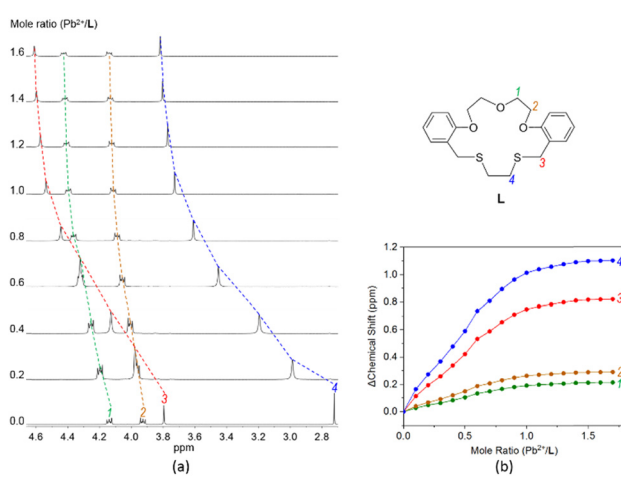


Fig. 3 (a) <sup>1</sup>H NMR titration of **L** ( $1.0 \times 10^{-3}$  M) with lead(II) perchlorate in  $\text{CDCl}_3/\text{CD}_3\text{CN}$  (v/v 1:1) and (b) titration curves for each proton in **L**.

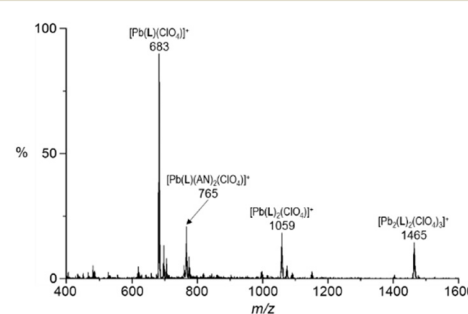


Fig. 4 ESI-mass spectrum of a mixture of **L** and  $\text{Pb}(\text{ClO}_4)_2 \cdot 3\text{H}_2\text{O}$  in  $\text{CH}_2\text{Cl}_2/\text{CH}_3\text{CN}$  (1:1, v/v).

## Data availability

The data supporting this article have been included as part of the ESI.†

## Conflicts of interest

There are no conflicts to declare.

## Acknowledgements

This work was supported by the NRF of Korea (2021R1C1C1006765, 2022R1A4A1022252 and RS-2023-00245420), COMPA (2024-24020010-11r, R&D Equipment Engineer Education Program), and the research fund of Chungnam National University.

## References

- 1 G. Chakraborty, I.-H. Park, R. Medishetty and J. J. Vittal, *Chem. Rev.*, 2021, **121**, 3751–3891.
- 2 M. Kim, J. Yi, S.-H. Park and S. S. Park, *Adv. Mater.*, 2023, **35**, 2203791.
- 3 J. Park, A. Adhikary and H. R. Moon, *Coord. Chem. Rev.*, 2023, **497**, 215402.
- 4 C. Bae, M. Gu, Y. Jeon, D. Kim and J. Kim, *Bull. Korean Chem. Soc.*, 2023, **44**, 112–124.
- 5 B. B. Rath, D. Kottilil, W. Ji and J. J. Vittal, *ACS Appl. Mater. Interfaces*, 2023, **15**, 26939–26945.
- 6 Z. Zheng, A. H. Alawadhi, S. Chheda, S. E. Neumann, N. Rampal, S. Liu, H. L. Nguyen, Y.-H. Lin, Z. Rong, J. I. Siepmann, L. Gagliardi, A. Anandkumar, C. Borgs, J. T. Chayes and O. M. Yaghi, *J. Am. Chem. Soc.*, 2023, **145**, 28284–28295.
- 7 J. Miao, W. Graham, J. Liu, E. C. Hill, L.-L. Ma, S. Ullah, H.-L. Xia, F.-A. Guo, T. Thonhauser, D. M. Proserpio, J. Li and H. Wang, *J. Am. Chem. Soc.*, 2024, **146**, 84–88.
- 8 I.-H. Choi, J.-M. Gu, H.-C. Kim, Y. Kim and S. Huh, *Bull. Korean Chem. Soc.*, 2023, **44**, 780–787.
- 9 A. H. Alawadhi, S. Chheda, G. D. Stroscio, Z. Rong, D. Kurandina, H. L. Nguyen, N. Rampal, Z. Zheng, L. Gagliardi and O. M. Yaghi, *J. Am. Chem. Soc.*, 2024, **146**, 2160–2166.
- 10 D. Kim, H. Yoo, K. Kim, D. Kim, K. T. Kim, C. Kim, J. Y. Kim, H. R. Moon and M. Kim, *Chem. Commun.*, 2022, **58**, 5948–5951.
- 11 J. Kim, C. Na, Y. Son, M. Prabu and M. Yoon, *Bull. Korean Chem. Soc.*, 2023, **44**, 507–515.
- 12 I. Hwang, S.-Y. Huang, S. Smith, V. Lynch, R. Custelcean, B. A. Moyer, N. Kumar, V. S. Bryantsev and J. L. Sessler, *J. Am. Chem. Soc.*, 2023, **145**, 14387–14394.
- 13 C.-H. Wang, Y.-C. Lin, S. Bhunia, Y. Feng, P. Kundu, C. L. Stern, P.-L. Chen, J. F. Stoddart and M. Horie, *J. Am. Chem. Soc.*, 2023, **145**, 21378–21386.
- 14 C. J. Pedersen, *J. Am. Chem. Soc.*, 1967, **89**, 2495–2496.
- 15 R. Rencsok, K. A. Jackson, T. A. Kaplan, J. F. Harrison and M. R. Pederson, *Chem. Phys. Lett.*, 1996, **262**, 207–212.
- 16 R. W. Saalfrank, N. Löw, S. Kareth, V. Seitz, F. Hampel, D. Stalke and M. Teichert, *Angew. Chem., Int. Ed.*, 1998, **37**, 172–175.
- 17 E. N. Ushakov, S. P. Gromov, O. A. Fedorova, Y. V. Pershina, M. V. Alfimov, F. Barigelli, L. Flamigni and V. Balzani, *J. Phys. Chem. A*, 1999, **103**, 11188–11193.
- 18 J. Kim, M. Shamsipur, S. Z. Huang, R. H. Huang and J. L. Dye, *J. Phys. Chem. A*, 1999, **103**, 5615–5620.
- 19 J. W. Steed, *Coord. Chem. Rev.*, 2001, **215**, 171–221.
- 20 S. P. Gromov, A. I. Vedernikov, N. A. Lobova, L. G. Kuz'mina, S. S. Basok, Y. A. Strelenko, M. V. Alfimov and J. A. K. Howard, *New J. Chem.*, 2011, **35**, 724–737.
- 21 A. Bey, O. Dreyer and V. Abetz, *Phys. Chem. Chem. Phys.*, 2017, **19**, 15924–15932.
- 22 H.-R. Yu, J.-Q. Hu, X.-H. Lu, X.-J. Ju, Z. Liu, R. Xie, W. Wang and L.-Y. Chu, *J. Phys. Chem. B*, 2015, **119**, 1696–1705.
- 23 I. Oral and V. Abetz, *Soft Matter*, 2022, **18**, 934–937.
- 24 R. M. Izatt, J. S. Bradshaw, S. A. Nielsen, J. D. Lamb, J. J. Christensen and D. Sen, *Chem. Rev.*, 1985, **85**, 271–339.
- 25 L. F. Lindoy, *The Chemistry of Macrocyclic Ligand Complexes*, Cambridge University Press, Cambridge, 1989.
- 26 G. W. Gokel, *Crown Ethers and Cryptands*, The Royal Society of Chemistry, 1991.
- 27 R. E. Wolf, Jr., J. R. Hartman, J. M. E. Storey, B. M. Foxman and S. R. Cooper, *J. Am. Chem. Soc.*, 1987, **109**, 4328–4335.
- 28 G. H. Robinson and S. A. Sangokoya, *J. Am. Chem. Soc.*, 1988, **110**, 1494–1497.
- 29 J. Buter, R. M. Kellogg and F. van Bolhuis, *J. Chem. Soc., Chem. Commun.*, 1991, 910–912, DOI: [10.1039/C39910000910](https://doi.org/10.1039/C39910000910).
- 30 A. J. Blake, G. Reid and M. Schröder, *J. Chem. Soc., Chem. Commun.*, 1992, 1074–1076, DOI: [10.1039/C39920001074](https://doi.org/10.1039/C39920001074).
- 31 Y. Jin, I. Yoon, J. Seo, J.-E. Lee, S.-T. Moon, J. Kim, S. W. Han, K.-M. Park, L. F. Lindoy and S. S. Lee, *Dalton Trans.*, 2005, 788–796, DOI: [10.1039/B415794J](https://doi.org/10.1039/B415794J).
- 32 M. Heller, *Z. Anorg. Allg. Chem.*, 2006, **632**, 441–444.
- 33 R. G. Pearson, *J. Am. Chem. Soc.*, 1963, **85**, 3533–3539.
- 34 S. Park, S. Y. Lee, K.-M. Park and S. S. Lee, *Acc. Chem. Res.*, 2012, **45**, 391–403.
- 35 E. Lee, S. Y. Lee, L. F. Lindoy and S. S. Lee, *Coord. Chem. Rev.*, 2013, **257**, 3125–3138.
- 36 S. Kim, L. F. Lindoy and S. S. Lee, *Coord. Chem. Rev.*, 2014, **280**, 176–202.
- 37 H. J. Kim and S. S. Lee, *Inorg. Chem.*, 2008, **47**, 10807–10809.
- 38 E. Lee and S. S. Lee, *Inorg. Chem.*, 2011, **50**, 5803–5807.
- 39 S. Kim, A. D. Siewe, E. Lee, H. Ju, I.-H. Park, K.-M. Park, M. Ikeda, Y. Habata and S. S. Lee, *Inorg. Chem.*, 2016, **55**, 2018–2022.
- 40 S. J. Lee, J. E. Lee, J. Seo, I. Y. Jeong, S. S. Lee and J. H. Jung, *Adv. Funct. Mater.*, 2007, **17**, 3441–3446.
- 41 C. S. Park, J. Y. Lee, E.-J. Kang, J.-E. Lee and S. S. Lee, *Tetrahedron Lett.*, 2009, **50**, 671–675.
- 42 H. Lee and S. S. Lee, *Org. Lett.*, 2009, **11**, 1393–1396.
- 43 E. Lee, H. Ju, I.-H. Park, S. Park, M. Ikeda, Y. Habata and S. S. Lee, *Analyst*, 2020, **145**, 1667–1676.
- 44 E. Lee, H. Ju, I.-H. Park, J. H. Jung, M. Ikeda, S. Kuwahara, Y. Habata and S. S. Lee, *J. Am. Chem. Soc.*, 2018, **140**, 9669–9677.

45 S. Kim, H. Ryu, J. K. Clegg, L. F. Lindoy and S. S. Lee, *Inorg. Chem.*, 2020, **59**, 15807–15812.

46 S. Kim, I.-H. Park, H.-B. Choi, H. Ju, E. Lee, T. S. Herring, J. Ding, J. H. Jung and S. S. Lee, *Dalton Trans.*, 2020, **49**, 1365–1369.

47 R. L. Davidovich, V. Stavila, D. V. Marinin, E. I. Voit and K. H. Whitmire, *Coord. Chem. Rev.*, 2009, **253**, 1316–1352.

48 R. L. Davidovich, V. Stavila and K. H. Whitmire, *Coord. Chem. Rev.*, 2010, **254**, 2193–2226.

49 R. Luckay, I. Cukrowski, J. Mashishi, J. H. Reibenspies, A. H. Bond, R. D. Rogers and R. D. Hancock, *J. Chem. Soc., Dalton Trans.*, 1997, 901–908, DOI: [10.1039/A605068I](https://doi.org/10.1039/A605068I).

50 L. Shimonov-Livny, J. P. Glusker and C. W. Bock, *Inorg. Chem.*, 1998, **37**, 1853–1867.

51 M. L. Golden, J. H. Reibenspies and M. Y. Darensbourg, *Inorg. Chem.*, 2004, **43**, 5798–5800.

52 I. Persson, K. Lyczko, D. Lundberg, L. Eriksson and A. Placzek, *Inorg. Chem.*, 2011, **50**, 1058–1072.

53 X. X. Wu, B. Ding, J. H. Li, P. Yang, Y. Wang and G. X. Du, *Inorg. Chem. Commun.*, 2013, **33**, 170–174.

54 H. Ju, E. Lee, S. Kim, I.-H. Park, J.-H. Lee and S. S. Lee, *CrystEngComm*, 2016, **18**, 2621–2625.

55 S. Mirdya, S. Roy, S. Chatterjee, A. Bauzá, A. Frontera and S. Chattopadhyay, *Cryst. Growth Des.*, 2019, **19**, 5869–5881.

56 Y.-M. Yang, C. Feng, Y.-H. Jiang, D.-H. Du, H. Zhao, G.-N. Zhang and Y.-C. Wang, *Transition Met. Chem.*, 2023, **48**, 55–61.

57 G. K. Kole, A. M. P. Peedikakkal, B. M. F. Toh and J. J. Vittal, *Chem. – Eur. J.*, 2013, **19**, 3962–3968.

58 J. S. Magyar, T.-C. Weng, C. M. Stern, D. F. Dye, B. W. Rous, J. C. Payne, B. M. Bridgewater, A. Mijovilovich, G. Parkin, J. M. Zaleski, J. E. Penner-Hahn and H. A. Godwin, *J. Am. Chem. Soc.*, 2005, **127**, 9495–9505.

59 <https://www.hyperquad.co.uk/hypnmr.htm>.